The role of eigen-stresses on apparent strength and stiffness of normal, high strength, and ultra-high performance fibre reinforced concrete

Awasthy, Nikhil; Schlangen, Erik; Hordijk, Dick; Šavija, Branko; Luković, Mladena

DOI
10.1016/j.dibe.2023.100277

Publication date
2023

Document Version
Final published version

Published in
Developments in the Built Environment

Developments in the Built Environment 16 (2023) 100277

Contents lists available at ScienceDirect

Developments in the Built Environment

journal homepage: www.sciencedirect.com/journal/developments-in-the-built-environment

The role of eigen-stresses on apparent strength and stiffness of normal, high strength, and ultra-high performance fibre reinforced concrete

Nikhil Awasthy [a], Erik Schlangen [b], Dick Hordijk [c], Branko Šavija [b], Mladena Luković [a,*]

[a] Engineering Structures, Delft University of Technology, Stevinweg 1, 2628, CN, Delft, the Netherlands
[b] Materials, Mechanics, Management & Design, Delft University of Technology, Stevinweg 1, 2628, CN, Delft, the Netherlands
[c] Adviesbureau Hageman, Polakweg 14, 2288, GG, Rijswijk, the Netherlands

ARTICLE INFO

Keywords:
Eigen-stresses
Strength
Stiffness
Concrete
High strength concrete
Ultra-high performance fibre reinforced concrete (UHPFRC)

ABSTRACT

Concrete is characterized in terms of its engineering properties, mainly strength and stiffness, which are subsequently used in structural design. However, the apparent (i.e., measured) concrete properties are not intrinsic but dependent on the conditions under which the measurement is performed. Herein a combined experimental and numerical study is performed to clarify the effects of hygral gradients and resulting eigen-stresses in self-restrained concrete on its apparent strength. Compressive strength, splitting tensile strength and Young's modulus are tested. Three mixes of varying strength grades are studied: normal strength, high strength, and ultra-high performance fibre reinforced concrete. Samples are subjected to two different curing conditions. To investigate the effect of size on the apparent properties, 50 mm, 100 mm and 150 mm cubes are tested. Depending on the size of the specimen there can be an underestimation or overestimation of up to 25% of the real concrete (e.g., splitting, direct tensile) strength.

1. Introduction

Concrete is the most consumed building material on the planet. Structural performance of concrete is governed by its strength and stiffness. Being a time dependent material, with volume changes and internal stresses developing even before the application of mechanical loading, understanding the development of the strength and stiffness over time is pivotal for its application.

The strength and stiffness of concrete increase with age when tested under standard curing conditions (i.e., moist curing at 20 °C). For other curing conditions, the compressive strength either remains constant or increases at a lower rate compared to moist cured conditions (Mehta and Monteiro, 2017). However, recent studies, especially related to the some innovative concrete types (Prinsse et al., 2020; Lantsoght et al., 2018), indicated that the strength and stiffness properties might decrease over time. A decrease in properties over time was reported for high strength concretes (Lantsoght et al., 2018) as well as for alkali-activated concrete (Prinsse et al., 2020). Lantsoght et al. (2018) reported a temporary decrease of the measured splitting tensile strength with time for a high strength concrete with strength grade C55/67. Prinsse et al. (2020) reported a decrease in the flexural strength, splitting tensile strength, and elastic modulus of two alkali activated concrete mixes when exposed to relative humidity (RH) of 50% after 28 days moist curing at 20 °C. This is in line with some previously reported results on alkali activated mixtures (Collins and Sanjayan, 2001; Wardhono et al., 2017). Maruyama et al. (2014) even reported a decrease in the compressive strength and stiffness over time for ordinary concrete exposed to different relative humidities ranging from 0% to 80% for a period of 5 months after being sealed cured for 2 months at 20 °C. The elastic modulus was reported to decrease over time even when specimens were exposed to a relative humidity in the range of 40–60%, which was attributed to micro-cracking (Maruyama et al., 2014).

Different studies highlighted the influence of parameters like the curing conditions, strength grade of concrete, and specimen size on the development of measured/apparent[1] strength and stiffness of concrete over time. With regard to the influence of curing conditions, Asselanis

* Corresponding author.
E-mail addresses: nikhil.awasthy@witteveenbos.com (N. Awasthy), erik.schlangen@tudelft.nl (E. Schlangen), hordijk@adviesbureau-hageman.nl (D. Hordijk), b.savija@tudelft.nl (B. Šavija), m.lukovic@tudelft.nl (M. Luković).

[1] The "strength" here is being referred to as the "apparent/measured" strength because the result may not represent the "real" strength due to the influence of the drying induced eigen-stresses, as discussed in this paper. Measuring strength merely based on the specific stress state due to mechanical loading, is the common way for determining concrete properties.

https://doi.org/10.1016/j.dibe.2023.100277
Received 14 September 2023; Received in revised form 31 October 2023; Accepted 13 November 2023
Available online 20 November 2023

et al. (1989) and Kocab et al. (2017) concluded that the continuously moist cured specimens have a higher elastic modulus than the specimens exposed to drying after an initial moist curing period. Regarding the compressive strength development, there are contradicting results with respect to the effect of curing. Carrasquillo et al. (1981) and Hameed (2009) reported higher compressive strength values for moist cured specimens relative to the specimens exposed to drying after an initial moist curing period. This is opposed to Iravani (1996) and Logan et al. (2009) who reported that drying resulted in a higher compressive strength value. Popovics (1986) and Bartlett et al. (Bartlett and MacGregor, 1994) attributed the temporary increase and decrease of the measured compressive strength to the influence of testing conditions. They highlighted that the non-uniform drying of the specimen could lead to moisture gradients, causing eigen-stresses due to self-restraint and resulting in a higher measured value of the compressive strength. Regarding tensile strength measurements, the influence of these eigen-stresses is reported to be different depending on the tensile test used: while drying after an initial moist curing period is reported to result in a higher splitting tensile strength compared to the continuously moist cured specimens (Hanson, 1968), specimens tested in direct tension showed lower strength upon drying (Bonzel and Walz, 1970). Drying has different influence on specimens with varying size. In case of moist cured conditions, the traditional size effect is prominent, i.e. smaller specimens have higher tensile and compressive strength. However, with the combination of air and water curing, it is reported (Soroka, 1994) that the final strength will be dependent on the interplay between the traditional size effect and the eigen-stresses caused by hygral gradients.

The complex interdependency amongst governing parameters, e.g., ongoing hydration, specimen geometry, boundary and environmental conditions in the test set-up, hygral gradients and the internal stresses, makes it challenging to clearly understand the underlying phenomena. Standard strength tests in laboratory, capture only the effect (i.e., the consequence) of eigen-stresses. In other words, experimentally we obtain only the load at which the specimen fails (i.e., the "measured strength"), but we are unable to *directly* measure the eigen-stresses and their distribution. As such, the effect of eigen-stresses that were present, could be missed if the testing frequency was not appropriate. So far, the role of eigenstresses is thoroughly studied in (massive) reinforced concrete structures. It is recognized that performance of these structures, durability and watertightness in particular, can be noticeably improved if in addition to conventional static design a rigorous hygro-thermal analysis is carried out (Alvaredo, 1995). The nonlinear FEM is the current gold standard for hygro-thermo-mechanical analysis (Sorgner et al., 2023; Bouquet, 2019). Similarly, for mechanical tests on material level, numerical models can be beneficial to clarify the interaction of mechanisms involved. By coupling eigen-stresses with the hygral gradients, the interaction between the "real" material strength, eigen-stresses distribution over time, and measured failure load can be better understood, and development of eigen-stresses over time can be estimated. This is essential for development of new types of concrete and advanced fabrication methods (e.g. 3D printing), where eigen-stresses might play an even larger role due to the large fraction of paste used, its different chemical composition, inclusion of fibres, additives and fine powders that affect transport and mechanical properties. For rigorous material testing and design it is important to understand and separate the role of eigenstresses from other underlying mechanism that might be measured in long-term tests (Prinsse et al., 2020; Bezemer et al., 2023; Wang et al., 2021). Therefore, in this paper, a combined experimental and numerical research has been carried out to investigate the measured strength and stiffness properties over time for three concrete mixes of varying strength grades. A commercial finite element tool (FEMMASSE), with coupled hydration (strength gain), transport, and mechanical behaviour, is used to continuously estimate the eigen-stresses and strength development, thereby providing deeper understanding of the experimental results.

2. Experimental study

2.1. Methodology

2.1.1. Materials and methods

The basis of the experimental plan is given in Fig. 1. The properties assessed experimentally include compressive strength, splitting tensile strength and elastic modulus up to an age of 155 days.

Three types of concrete mixes were designed: (i) Normal Strength Concrete (NSC), with a water-to-cement ration (w/c) of 0.6, (ii) High Strength Concrete (HSC) with w/c of 0.45, and Ultra High Performance Fibre Reinforced Concrete (UHPFRC) with w/c of 0.23. The details of the mix design are shown in Table 1. The 28 days cube strength of NSC, HSC and UHPFRC were 25 MPa, 67 MPa, and 120 MPa, respectively.

To investigate the size effect due to drying, 50 mm, 100 mm and 150 mm cube specimens were tested in splitting tension and compression. As the aim of the tests was to capture the governing mechanisms, the effect of specimen size was studied only for NSC. Although for HSC and UHPFRC, the hygral diffusivity parameters, and thereby the drying speed, are different compared to NSC, the governing mechanisms are expected to be the same.

2.1.2. Specimen preparation and curing

The NSC mix was prepared in two batches of 100 L whereas the HSC and UHPFRC mixes were prepared in single batches of 65 L. In general, the casting procedure of all the mixes are similar, with adjustments for the UHPFRC mixes.

For the mixing process, a concrete mixer of 100 L capacity was used. The mixing of NSC and HSC consisted of initial dry mixing of sand and gravel for 3 min followed by the addition of cement and additional mixing for 1 min. Subsequently, water and superplasticizer were added and mixed for 3 min. In case of UHPFRC, additional ingredients like silica fume and blast furnace slag were mixed with sand and gravel particles followed by the addition of cement and subsequently mixed for 3 min. Then superplasticizer mixed with water was added, followed by addition of steel fibres and subsequent mixing for 4 min. Mixtures were then poured in moulds, in three layers each followed by a constant vibrations for 20 s. Specimens were demoulded after 24 h and then placed in the fog room and maintained at 22 °C and 99% RH for 28 days. After the 28-day curing period, some specimens were taken out and kept at 20 °C and 55% RH before being tested (28 Day Moist curing regime, labelled as 28DM). Others were left in the fog room until the period of 91 days (Continuous Moist curing regime, labelled as CM).

2.1.3. Mechanical tests

The strict control and procedure for conditioning of samples prior to testing is of utmost importance for 'controlling' the eigen-stresses and enabling reproducible measurement of strength. Since in NEN12390 it is only mentioned to keep the surface dry, with no specific duration, the procedure from previously conducted experiments (Prinsse et al., 2020; Luković et al., 2017a) was adopted in this study. Prior to testing, and after removing them from the fog room, specimens were kept in the lab conditions (20 °C and 55% RH) for 2 h. For the mixes moist cured for 28 days and subsequently exposed to drying, the compressive strength, splitting tensile strength and elastic modulus were determined at the ages of 28, 56, 91 and 155 days. For specimens continuously moist cured, the above properties were determined at 28 and 91 days.

The elastic modulus was determined using 100 × 100 × 400 mm^3 prisms according to the ISO 1920-10-2010 standard with the exception that the prisms were not reimmersed in water for 12 h before testing. The test was performed using the TONI-BANK machine with the speed of 1.6 kN/s (load control testing). The compressive and splitting tensile strength tests were done on three sizes of cube specimens, having dimensions 50 mm, 100 mm and 150 mm. The 150 mm and 50 mm cubes were directly taken out of the fog room, whereas the 100 mm cubes were wet sawn from the prisms of 100 × 100 × 400 mm^3. The cubes were

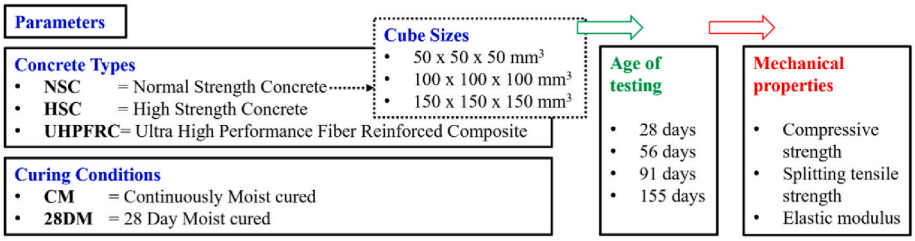

Fig. 1. Overview of the experimental plan.

Table 1
Mix design details.

Ingredients	NSC (kg/m^3)	HSC (kg/m^3)	UHPFRC (kg/m^3)
CEM I 42.5 N	260	–	70
CEM I 52.5 R	–	367	800
Blast furnace slag	–	–	104
Silica fume	–	–	44
water	156	167	205
sand 0.125–0.25 mm	79	75	213
sand 0.25–0.5 mm	256	93	319
sand 0.5–1 mm	256	150	529
sand 1–2 mm	158	223	–
sand 2–4 mm	99	300	–
gravel 4–8 mm	394	373	–
gravel 8–16 mm	729	653	–
superplasticizer (Glenium)	0.26	5	27
steel fibres (13 mm)	–	–	125

subsequently left for 2 h in the lab conditions before testing. The tests were done using the CYBERTRONIC machine. Standard NEN-EN-12390-3 was followed for compressive test, whereas the splitting tensile strength test was done according to NEN-EN-12390-6 standard except that instead of cylindrical specimens, cube specimens were used. All results (mean and standard deviations) are based on three tested specimens.

3. Experimental results and discussion

3.1. Influence of curing conditions and age

3.1.1. Compressive strength

Fig. 2 show the measured compressive strength for the three types of concrete using 100 mm cubes. For the 28-day moist cured samples (28DM), the strength for the UHPFRC mix increases continuously with time with an increase of 24% at 155 days relative to 28 days. In case of the NSC and HSC mixes, both show an initial increase followed by a slight decrease of the average strength within the period of 91–155 days. At the age of 155 days, the compressive strength of both mixes is still higher than that measured at 28 days.

At 91 days, there is not much difference between the values of CM and 28DM samples for HSC and UHPFRC specimens (within 5% difference). For NSC specimens, continuously moist cured samples (i.e., CM series) are 16.8 % stronger than those exposed to drying (i.e., 28DM series).

3.1.2. Splitting tensile strength

The splitting tensile strenght for the three types of concrete over time is shown in Fig. 3. For the 28DM cured samples, the splitting tensile strength for NSC specimens is increasing, with the increase of 24 % at the age of 155 days, relative to 28 days. In case of the HSC specimen, the strength is almost constant over time. However, for the UHPFRC specimens, measured splitting tensile strength is reducing within the period from 56 to 155 days with a decrease of around 9% at the age of 155 days relative to the 28-day value. The compressive strength measurements of UHPFRC did not show decrease. On contrary, unlike with NSC and HSC, they showed the continuous compressive strength increase.

At 91 days CM and 28DM samples show similar splitting strength values, both for NSC and HSC. However, for UHPFRC specimens, 28DM samples give 10% higher results than CM ones. It is also observed that under continuous moist curing, UHPFRC cubes exhibited strength reduction by 9% from 28 days to 91 day. Note that UHPFRC exhibited larger variability in results compared to HSC and NSC, which is commonly observed for fibre reinforced concrete.

With UHPFRC, there is a more pronounced apparent splitting strength increase (especially at 56 days) compared to NSC and HSC. UHPFRC has lower diffusion coefficient, owing to its denser microstructure, so it requires longer time to reach the hygral equilibrium and is subjected longer to eigen-stresses. Towards reaching the equilibrium, and provided that no (significant) microcracking occurs, the effect of eigen-stresses is reduced and apparent splitting strength is therefore decreasing and approaching the “intrinsic” strength. This decrease happens if the effect of eigen-stresses, causing a lower apparent strength, overwins the strength development at later ages.

3.1.3. Elastic modulus

The measured elastic moduli for the three concrete types are given in Fig. 4a. The moduli increase with age for all concrete types, irrespectively of the type of curing. For 28DM samples at 155 days, the highest increase relative to 28 days strength is seen for the NSC (12%)

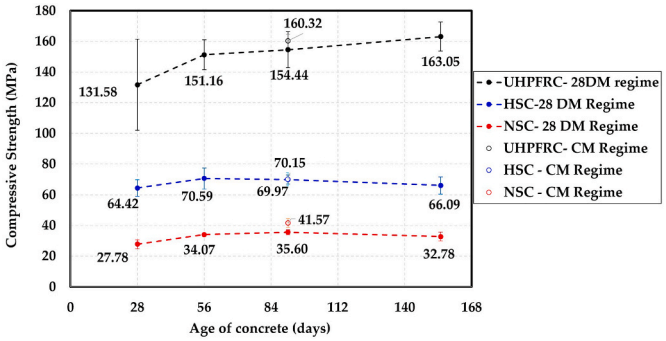

Fig. 2. Development of (apparent) compressive strength with age.

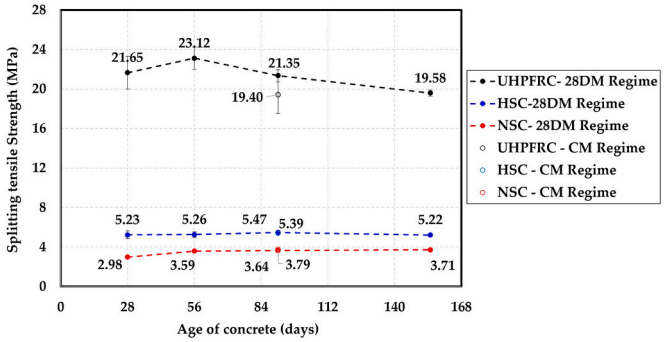

Fig. 3. Development of (apparent) spitting tensile strength with age.

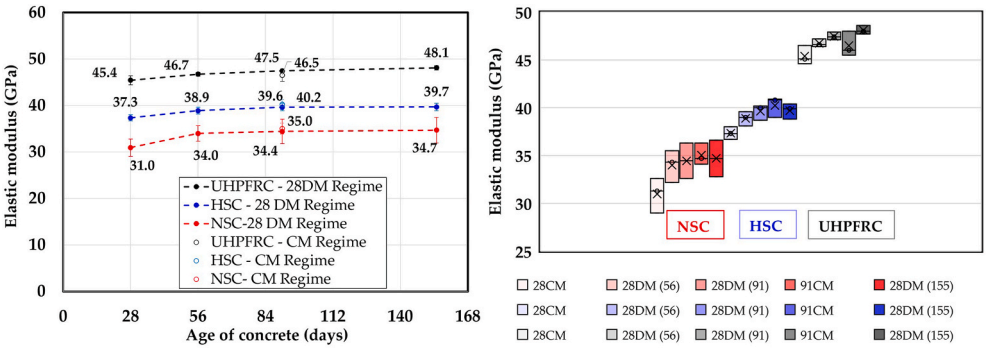

Fig. 4. (a) Development of Elastic modulus with age and (b) statistical representation of measurements.

followed by HSC (6%) and UHPFRC (5%). At 91 days, there is not much difference between the values of CM and 28DM samples for all the concrete types, indicating that drying conditions do not significantly influence the measured elastic moduli for all the studied concrete types and testing ages.

In Fig. 4b, the variability of elastic moduli data is shown. It can be observed that for the samples exposed to drying, NSC concrete shows larger elastic modulus variability compared to HSC and UHPFRC. Also in UHPFRC, dry samples on average have higher elastic modulus and smaller variability compared to wet samples, whereas this is not obvious for NSC and HSC.

3.2. Influence of specimen size

3.2.1. Compressive strength test

In Fig. 5 the compressive strength of normal strength concrete obtained by testing 50 mm, 100 mm, and 150 mm cube specimens is shown. Note that generally concrete specimens and structures of larger sizes show lower strength (Bažant, 2000), and different theories have been put forward to explain this size effect (Grassl and Bažant, 2009; Carpinteri, 1994; Van Vliet and Van Mier, 2000). Herein, we refer to this phenomenon as a "traditional size effect", to differentiate from other factors which may influence the measured mechanical properties, most notably the occurrence of eigen-stresses.

Compressive strength of 50 mm and 150 mm CM cubes follow the traditional size effect (i.e., smaller specimens show higher strength) (Fig. 5b). This is expected, as there are presumably no hygral gradients and consequently no eigen-stresses present in these specimens. The 100 mm cubes do not clearly follow the traditional size effect, but variations lie within experimental scatter. On the other hand, 28DM specimens show more complex behaviour (Fig. 5a). First the general trend, being an increasing strength with age is found, after which the compressive strength remains almost constant, or even decreases for 50 mm and 100 mm specimens. In case of the 150 mm specimens, the strength only "increases". This can be because it takes longer time for larger specimen to reach the hygral equilibrium, meaning that the measured strength gain is not reflecting the "real" material strength but only the effect of eigen-stresses. The traditional size effect is not dominant for some testing ages: even more, at 155 days the largest specimen has the highest compressive strength of the three specimen sizes tested.

3.2.2. Splitting test

In Fig. 6 the splitting tensile strenght of Normal Strength Concrete for different specimen sizes is shown. For both curing regimes and all testing ages, the measured splitting strength is higher for the smaller specimen dimensions, in line with the traditional size effect. In the smallest samples, a steep trend of strength increase (up to 56 days) and decrease (between 56 days and 91 days) is captured: splitting strength at 56 days is around 25% higher compared to that at 91 days. Therefore, depending on the moment of testing and the hygral gradients present, the measured properties can be up to 25% inaccurate (overestimated in this case). Note that the scatter in measurements is relatively low, so this difference cannot be (only) a statistical effect. 100 mm and 150 mm cubes showed only strength increase within the measured period and testing frequency.

3.3. Discussion of experimental results

Varying curing conditions cause hygral gradients that lead to the development of time-dependent eigen-stresses which influence the measured material properties (Bonzel and Walz, 1970). Hygral gradients are affected by the initial moisture state, environmental conditions, geometry of the specimen and diffusivity properties of concrete. As a result it is complex to evaluate the positive and negative effects of drying (Conroy-Jones and Barr, 2004). Although it is difficult to make clear conclusions based on experiments alone, also given the fact that some of the measured variations lie within experimental scatter, some general trends can be observed.

One of major differences between the studied NSC, HSC, and UHPFRC is their w/c ratio, which is related to porosity and determines

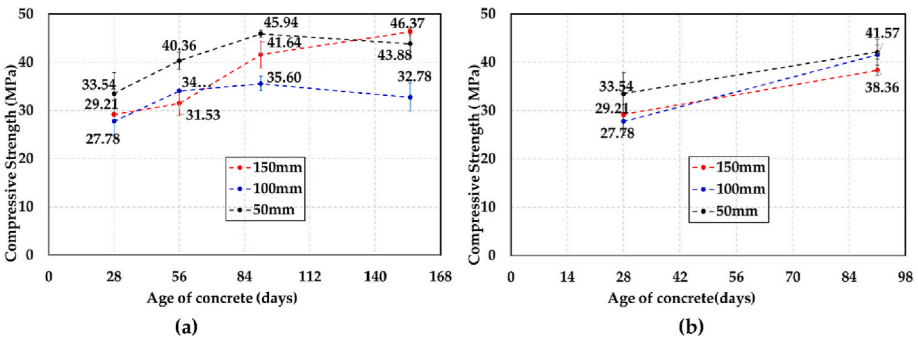

Fig. 5. Development of compressive strength of NSC mixes for **(a)** 28DM Regime **(b)** CM Regime.

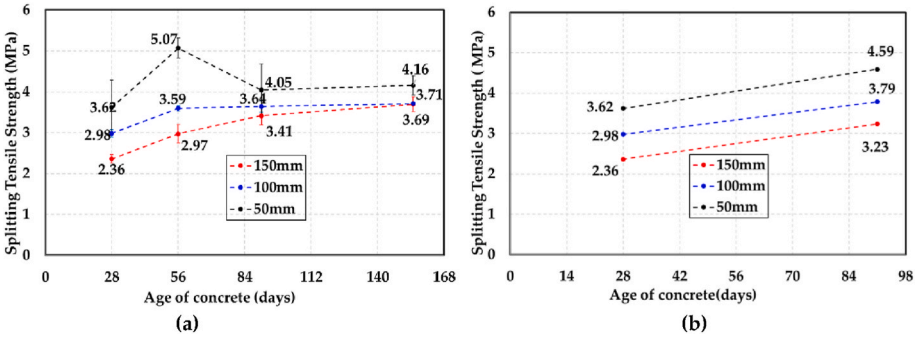

Fig. 6. Development of splitting tensile strength of the NSC mix for different specimen sizes for **(a)** 28DM Regime **(b)** CM regime.

the mechanical (Birchall et al., 1981; Liu et al., 2017) and the transport (Zhang and Zhang, 2014) properties of concrete. While the influence of w/c on the mechanical properties is reflected by the measured strength under continuous moist curing conditions, the impact of w/c ratio on the specimens exposed to drying is more complex. As shown in (Luković et al., 2017b), w/c ratio determines the drying rate of concrete, which affects the hydration reaction and therefore the further strength gain. Consequently, the three studied concretes will differ both in terms of (i) hygral gradients and time required to reach hygral equilibrium with the environment, and (ii) the role that drying (moisture loss) has on the strength development.

With respect to different sizes of the specimens, whenever hygral gradients are present, the measured (i.e., apparent) strength depends on the interplay between drying and the traditional size effect. Soroka et al. (Soroka, 1994) argued that there is a greater negative effect of drying on the measured strength value for smaller specimens as they have a larger volume of outer affected zones with respect to the entire volume. This is probably true if microcracks do occur because of drying shrinkage. Note that in the current study, surface imaging of the specimens using a portable microscope was performed to investigate possible cracking due to eigen-stress and microcracks could not be observed. Still, even if no microcracking occurs, drying shrinkage will cause eigen-stresses. Surface exposed to drying is under tension, while the core of the specimen is under compression, with the exact stress distribution dependent on the moisture gradient in the specimen. Depending on this eigen-stress distribution and the loading conditions, drying can sometimes temporarily (if no microcracking occurs) increase the measured compressive strength. Once the moisture distribution in the specimen is uniform, the influence of eigen-stresses on the measured strength disappears.

In Fig. 7 comparison of measured compressive strength and tensile splitting strength for two curing regimes is presented. As expected, in smaller samples the role of eigenstresses is higher. But in larger samples, eigen-stresses are longer present as it takes longer to reach the hygral equilibrium. Therefore, the continuous strength increase measured in 150 mm sample is only the effect of eigen-stresses and, if not properly considered, can wrongly overestimates the "real" material strength. It seems also that the compressive strength test is for longer time susceptible to moisture gradients compared to the splitting tensile strength test, but also the influence of eigen-stress on strength increase/decrease is lower. Even more, for the same testing period (from 56 to 90 days), whereas the measured compressive strength is increasing, the splitting tensile strength is decreasing. This is merely the effect of eigenstresses and not the real material strength increase/decrease. Similar is observed for the measured compressive and splitting strength of UHPFRC between 56 and 155 days.

Measured strengths in the current study are compared with the literature. Splitting tensile strength is in line with Hanson's results (Hanson, 1968), having a mix with a similar water-to-cement ratio (Fig. 8). Drying after 28 days does not significantly influence the measured splitting tensile strength at the age of 91 day. Furthermore, also the ratio between the compressive strength with 28DM curing regime and CM curing regime is compared to literature findings (Table 2). In case of the NSC mixes, Carrasquillo et al. (1981) and Ozer

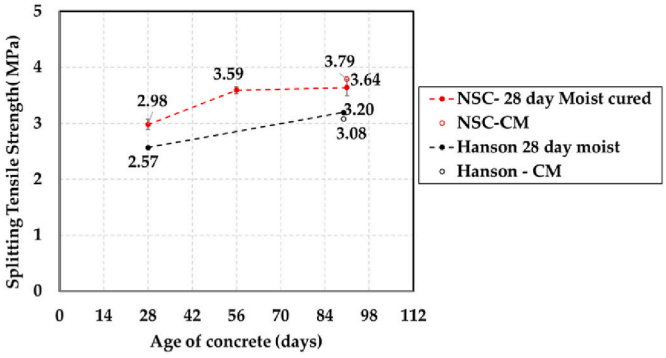

Fig. 8. Development of splitting tensile strength obtained in this study compared to Hanson (Hanson, 1968).

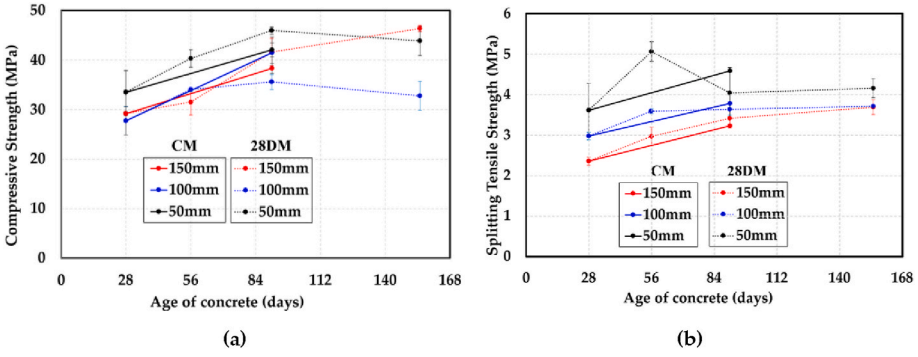

Fig. 7. Comparison of (a) compressive strength and (b) tensile splitting strength for two curing regimes.

Table 2
Compressive strength ratio between 28DM regime and CM regime for NSC and HSC.

Moist Curing period (days)	$R_{NSC} = f_{c,\ cube,\ 28DM}/f_{c,\ cube,\ CM}$				$R_{HSC} = f_{c,\ cube,\ 28DM}/f_{c,\ cube,\ CM}$				
	Drying period (days)	Carrasquillo C30 w/c = 0.7	Ozer C25 w/c = 0.7	This study C20/25 w/c = 0.6	Drying period (days)	Carrasquillo C70 w/c = 0.32	Hameed C60 w/c = 0.32	Iravani C65 w/c = 0.4	This study C55/67 w/c = 0.45
0–28					28–56			1.12	
0–28	28–91	0.99	1.05	0.93	28–91	0.96	0.98	1.25	1.0
0–28	28–180			0.98	28–147			1.21	

and Ozkul (2004) reported similar ratios (0.99 and 1.05) which are in line with this study (0.93). The current NSC mix has a lower water-to-cement ratio compared to aforementioned studies (0.6 vs. 0.7 for (Carrasquillo et al., 1981; Bezemer et al., 2023)). For the current HSC mix, at 91 days, the compressive strength is the same for the samples cured under 28DM and CM regimes. This is in accordance with studies in which w/c of 0.32 was used (Carrasquillo et al., 1981; Hameed, 2009), resulting in a slightly lower compressive strength of specimens exposed to drying. On the other hand, Iravani (1996) reported an opposite trend in HSC with a w/c = 0.4: an increase in "apparent" compressive strength of 25% for specimens exposed to drying at 91 day.

Although general trends may be compared, a direct comparison between the current study and some of the publications discussed above is difficult due to different specimen sizes: while Hameed (2009) used specimens of the same shape and size (i.e. 100 mm cubes), Carrasquillo and Iravani (Carrasquillo et al., 1981; Iravani, 1996) used cylinders (100 mm diameter, 200 mm height). The shape and the size of specimens (and the ratio of volume to sample surface) has a high effect on the non-uniform drying, and, consequently, the distribution of eigen-stresses (Zhang and Hubler, 2020).

Regarding the elastic modulus, the measured properties are almost constant, and drying conditions seems not to have the influence: CM regime is comparable to 28DM regime at 91 days, for all the three concrete mixes (Table 3 and Fig. 4). The results on HSC mix are consistent with those of Asselanis et al. (1989), of a similar water-to-cement ratio (0.23 vs 0.3).

The results of the current study are compared with the results reported by Soroka et al. (Soroka, 1994) for the compressive strength of different specimen sizes measured at 28 and 90 days (Fig. 9). For moist cured specimens at 28 days, both (Soroka, 1994) and the current study (regimes D and E in Fig. 9a) show a traditional size effect, i.e. decrease of strength with increase in specimen size. This is also in line with observations for continuous water curing samples from (Soroka, 1994) and current study at 90 days (regimes D and F in Fig. 9b). Again, this is expected, as no hygral gradients (and eigen-stresses) are present, so only the traditional size effect plays a role. Comparable results are also observed at 28 days in regime C (6 days water cured samples of Soroka et al. (Soroka, 1994)) which, although showing the drying effects on the smallest size samples, generally follow the traditional size effect.

At 90 days, regimes C and E (Fig. 9b), indicating 6 days water cured samples of Soroka et al. (Soroka, 1994) and 28 days moist cured samples of the current study, respectively, show clearly difference from the traditional size effect. In the extreme case of no curing, Soroka et al. (Soroka, 1994) show even the reverse effect from the traditional size effect, for both testing ages of 28 and 90 days.

In general, significant differences in apparent compressive strength can be observed for specimens exposed to drying, where the eigen-stresses clearly influence the development of apparent compressive/tensile splitting strength. Therefore, it is of utmost importance to properly consider the influence of specimen size and eigen-stresses on measured properties otherwise material properties might be largely inaccurate.

Table 3
Comparison of Elastic modulus for both CM and 28DM regimes at 91 days.

Concrete Type	E_{CM}		E_{28DM}		E_{CM}/E_{28DM}
	Mean	SD	Mean	SD	
NSC	35.0	2.6	34.4	1.2	1.07
HSC	40.2	1.1	39.6	0.8	1.01
HSC Asselanis (Asselanis et al., 1989)	43.4		42.1		1.03
UHSC	46.5	1.3	47.5	0.4	0.98

4. Numerical study

4.1. Introduction of the model

The numerical tool used in this study is FEMMASSE-MLS (version 8.5). FEMMASSE is a 2D Finite Element software specifically designed for concrete material specialists. The software consists of 4 main parts: hydration, hygral and thermal properties, and the mechanical behaviour, which are coupled. In the context of this work, FEMMASSE allows calculating hygral behaviour (diffusion, drying, etc.) and the mechanical behaviour (i.e., response to internal or external loads). In other words, the drying process and resulting eigen-stress can be simulated: with changing moisture content stresses are introduced, as there is a relation between moisture change and strain. This allows insight into the development of material properties and eigen-stresses depending on specific material composition and characteristics. Furthermore, the model allows one to independently study the influence of individual parameters, which is experimentally very challenging. The focus in this study is restricted to simulating tensile tests: splitting tensile, direct tensile and flexural strength test. The effect of drying induced eigen-stresses on the measured compressive strength cannot be studied because the model cannot simulate compressive failure. The results of the splitting tests are compared with the experimental results, whereas the results of direct tensile and flexural strength tests are compared with trends reported in literature for the influence of testing condition on the apparent strength. The model is configured to consider the effect of hydration (increase in "real" mechanical properties over time) and hygral behaviour and gradients due to drying. The effects of self-desiccation, relaxation and heat are assumed to be negligible and are therefore not considered in the presented simulations. Note that a staggered flow-stress analysis is performed: eigen-stresses and possible microcracking are result of hygral gradients but there is no influence of microcracking on the moisture transport. This is a reasonable assumption as drying shrinkage microcracks seem not to have a significant effect on drying rate of mortars and concrete (Bisschop and van Mier, 2008).

4.2. Approach and workflow

Material strength parameters for different types of concrete, under continuously moisture cured conditions (CM), were deduced from experimental results. Therefore, these tests are assumed to yield the "real" material properties, i.e., not affected by eigen-stresses caused by hygral gradients. The approach/workflow to fulfil the modelling objectives is further described.

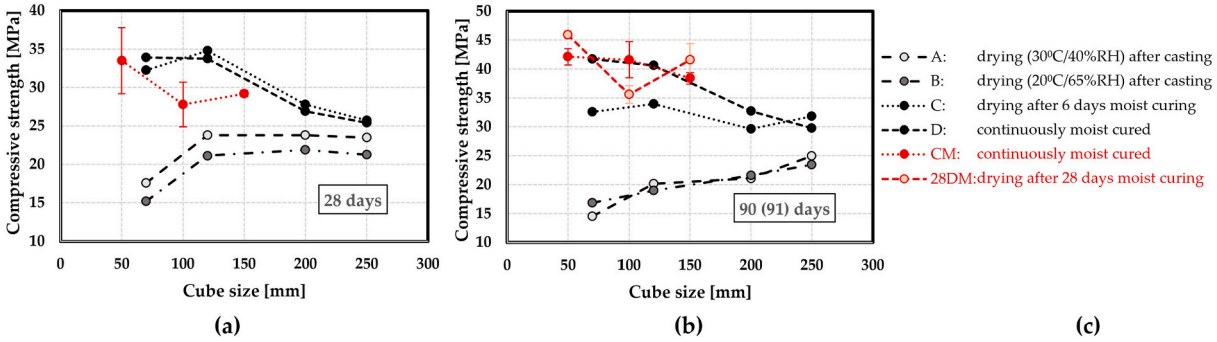

Fig. 9. Compressive strength of various regimes and specimen sizes in the current study (red) compared to results of Soroka et al. (Soroka, 1994) (black) at (a) 28 days, (b) 90 (or 91) days with (c) corresponding legend.

4.2.1. *Assigning the material properties*

In the model, the hydration and hardening of concrete is considered through the maturity concept (Roelfstra, 1989; Saul, 1951). As tests under these conditions were performed until the age of 91 days, the strength parameters were assumed to be constant after 91 days. A value of 0.2 is adopted for Poisson's ratio. For the tensile softening behaviour, Hillerborg's bilinear curve (Hillerborg, 1978) defined in FEMMASSE is adopted with model parameters given in Table 4. A smeared crack model is used.

4.2.2. *Assigning hygral properties*

In the laboratory, after 28 days of moist curing, specimens were placed in a chamber with a controlled environment (50% RH and 20 °C) and exposed to drying from all sides. Due to the two-dimensional nature of the FEMMASSE software, the real exposure conditions have been simplified in the model. All specimens were therefore simulated as two-dimensional (2D). The hygral behaviour was incorporated by defining a hygral boundary on all four (in plane) sides of the specimens and specifying 50% as the relative humidity of the environment. The diffusion, film, and shrinkage coefficients (Table 5) were also considered in order to simulate the flow of the moisture within the concrete specimen, causing differential shrinkage and the eigen-stresses. A governing partial differential equation used for modelling moisture transport in 1D is:

$$\frac{\partial H}{\partial t} = \frac{\partial}{\partial x}\left(D(H)\frac{\partial H}{\partial x}\right) \tag{1}$$

where H is the relative humidity and $D(H)$ is a humidity dependent diffusion coefficient. The diffusion coefficient is given as follows (Bazant, 1986):

Table 5
Hygral parameters used in numerical simulations.

Type of concrete	D_0 [m^2/h]	a [−]	h_c [−]	Film coefficient [mm/day]
NSC	99×10^{-8}	0.2	0.792	3.5
HSC	19.82×10^{-8}	0.2	0.792	0.7

$$D(H) = D_0\left[a + \frac{1-a}{1+\left(\frac{1-h}{1-h_c}\right)^4}\right] \tag{2}$$

The parameters are determined by calibration with experimental results reported in literature. The diffusion curve for normal strength concrete is based on experimental results from Bažant (Bazant, 1986) and are given in Table 5. For high strength concrete, due to the lack of information in the literature, a five times lower diffusion coefficient is assumed. Due to the absence of experimental data, the hygral response of UHPFRC was not simulated.

4.2.3. *Geometrical properties and applied boundary conditions*

All simulations were performed in 2D using regular plane stress elements. The shape and dimensions of the specimens are based on the specific experimental setup (Fig. 10).

For simulating the splitting tensing test, a 2D model was made for the different cube sizes. The load is applied on the wooden block at the centre of the specimen, being also supported by a wooden block from the bottom. For the flexural strength, specimens with height of 100 mm and length of 500 mm were modelled. Three steel plates of size 25 × 5 mm2 were simulated, two acting as supports and one as a loading point. In the splitting test, wooden blocks were used, similar to the experiment. The wood and steel used were modelled as linear isotropic. In case of the

Table 4
Tensile softening properties for NSC at different age used as input in the numerical simulations.

Stress-crack width relation used in the model (Hillerborg, 1978)	days	f_t [MPa] tensile strength	c [−] coefficient	s [MPa] stress at the breakpoint	w_1 [mm] crack at the breakpoint	w_2 [mm] stress-free crack
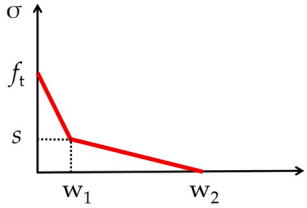	28	2.68	0.2	c × f_t	0.05	0.23
	56	3.23				
	91	3.41				
	155	3.41				

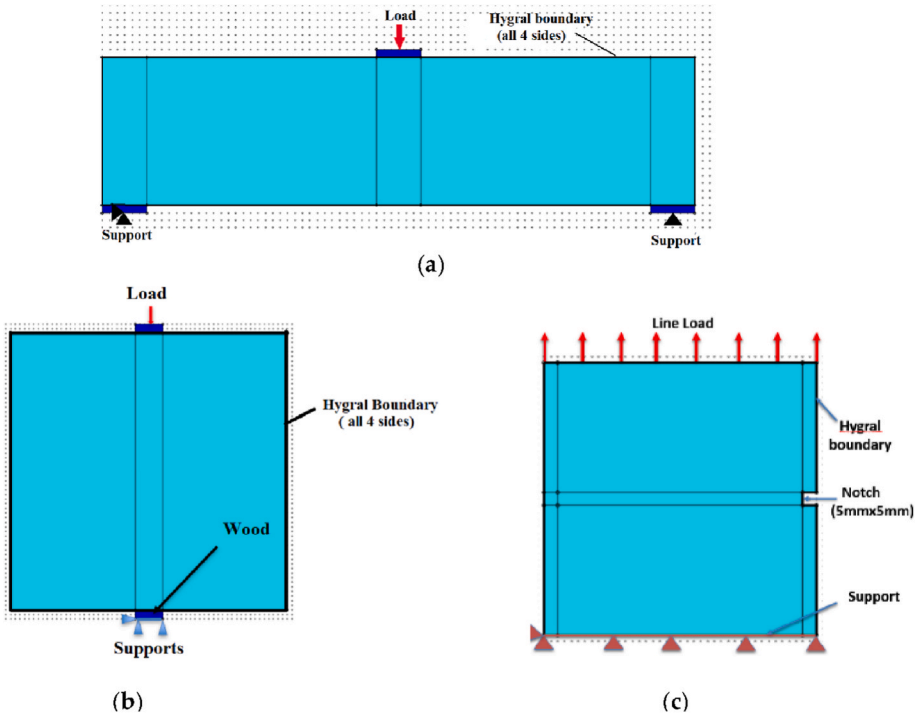

Fig. 10. Geometry and boundary conditions of the model for: (**a**) Flexural test (**b**) Splitting test (**c**) Direct tensile test.

direct tension test, a model of 100 × 100 mm^2 was made with a notch (5 mm × 5 mm) at the edge and subjected to a line load applied at the top. Note that in these tests, beside hygral effects, the notch would also create bending.

4.3. Validation of the hygral behaviour

For the validation of the FEMMASSE model, the hygral behaviour for NSC specimens and the humidity profile across the specimen, based on the experimental results published by Hanson (1968), were simulated first. The diffusion parameters published by Bažant (Bazant, 1986), based on the same experiments of Hanson (1968), were used. Although the specimens used by Hanson were cylindrical as opposed to cubes used in this study, it was found that this would not significantly affect the results in terms of moisture distribution (Fig. 11a). Note that for the film coefficient (which defines the convective boundary condition), a sensitivity analysis was performed resulting in the best fit value of 3.5 mm/day.

Specimen with hygral gradients was then subjected to the tensile splitting strength of concrete. The numerical predictions were compared to the splitting tensile strength measurements of Hanson (1968). As a result of eigen-stresses due to drying, an increase in (apparent) strength at 90 and 180 days was found, similar to the experiments (Fig. 11b).

4.4. Influence of eigen-stresses

4.4.1. Splitting test

The splitting tensile tests are simulated for the three specimen sizes - 150 mm, 100 mm, and 50 mm for both the NSC and HSC mixes. The simulated curing regimes are the same as in the experiments - Continuously Moist (CM) cured and drying after 28 Days Moist curing (28DM). The input hygral properties as discussed above are used. The experimental results from CM regime are directly used as input mechanical properties (i.e., no hygral gradients). For periods larger than 91 days, for which no experimental data was available, it is assumed that the properties are constant. Fig. 12 shows the difference between numerically simulated splitting tensile strength of CM and 28DM samples. The similar apparent strength increase is observed as in Fig. 11b. Drying after the 28-day moist curing period leads to increase in the measured splitting tensile strength over time as compared to the continuously moist cured samples. Smaller the cube, larger the difference between the apparent and real strength. The use of numerical simulation makes it possible to consider longer curing periods, so the simulations were extended up to 50 years. Eventually the hygral equilibrium is reached and DM and CM curing regimes reach the same strengths.

To understand better the underlaying mechanisms and their interaction, the behaviour of 100 mm specimen is investigated in detail. Non-

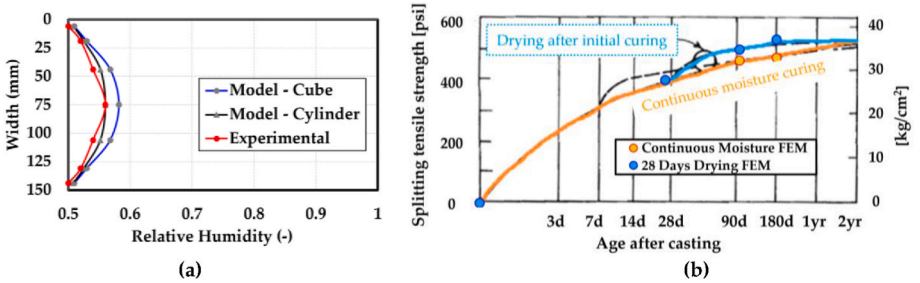

Fig. 11. (a) Variation of relative humidity along width based on cube/cylindrical cross sections **(b)** Development of (apparent) splitting tensile strength in the numerical study and Hanson (adapted from (Hanson, 1968)).

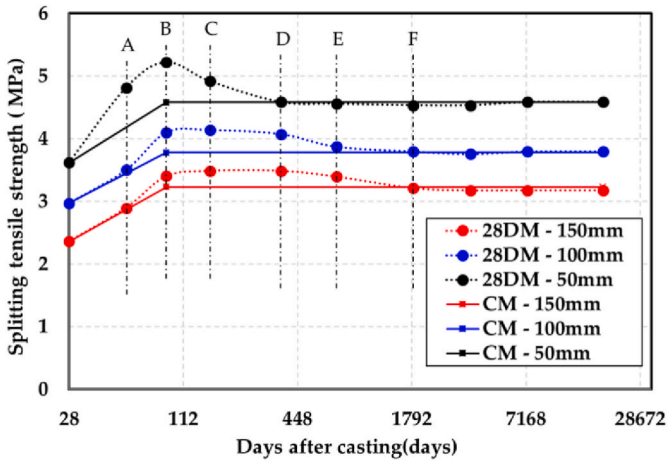

Fig. 12. Apparent splitting tensile strength with time for Normal Strength concrete (NSC) specimens. A, B, C, D, E and F corresponds to 56 days, 91 days, 155 days, 1 year, 2 years and 5 years.

uniform drying causes hygral gradients (i.e. differences in internal relative humidity) in the specimen (Fig. 13a). Especially in the initial period, there is a high gradient in relative humidity along the specimen, resulting in high tensile stresses at the surface (around 1/5 of the cube size is under tension) and compressive eigen-stresses at the core (Fig. 13b). Stresses reduce over time, towards reaching hygral equilibrium. At the surface of the specimen the material enters the post-peak regime in tension (i.e., the softening regime) (Fig. 13c), so drying causes microcraking.

Contrary to drying, splitting load (Fig. 14a) results in a compressive zone just underneath the point load and support (around 1/20–1/10 of the cube size), and tensile zone in almost entire core of the specimen (Fig. 14b and c).

Stress distributions due to splitting and drying load in linear elastic stage are sketched in Fig. 15a, b and c. Note that there is a critical zone, just below the surface layer, where drying will cause additional tensile stress, on top of that caused by splitting (Fig. 15d). These zones (top 5–15 mm and bottom 85–95 mm) are the zones where microcracking due to drying was also observed. As a result, the failure load in splitting test is affected by the additional tensile stresses close to surfaces and the compressive stresses at the core caused by drying. For this specific loading (splitting tensile test) and environmental conditions, it seems that compressive stresses are governing: similar as with prestressing, they delay the failure and lead to higher measured (apparent) splitting strength.

Simulated results for NSC are compared to experimentally measured (Fig. 16). Although, the general trend seems to be well predicted numerically, the magnitude and timing of increase and decrease for different sizes seems to be different in experiments and simulations. The numerical model reproduced the experimental trend accurately for 150 mm specimens throughout the observed period. While a similar trend is observed for 50 mm specimens, there seems to be a shift in timing. The rapid increase at the 56 days as shown by the experimental results is also captured numerically. However, at later stages, the model predicts slower drying and a more gradual decrease of the splitting tensile strength compared to the experiments. For the 100 mm specimens, the model follows the experimental trend until 56 days, but subsequently the model predicts slower drying compared to the experiment.

The differences in experimental and modelling results might be due to the assumptions taken in the model (e.g., related to hygral coefficients that were not directly measured, or relaxation of eigen-stresses that is neglected), as well as the fact that drying is simulated in 2D while in reality it happens from all six sides of the specimens. Nevertheless, for all specimens, similarly as in experimental study, the model shows that depending on moment of testing, measured properties can be up to 25% higher compared to the "real" material strength if the role of eigen-stresses is not considered. Although there are differences, it is observed that the model can predict the general trend in which drying after 28DM regime increases the splitting strength in the initial period followed by the decrease and finally the stabilizing effect at the later stages.

To understand the trend with respect to different size specimen, stress development in 50 mm, 100 mm and 150 mm cubes is analysed in detail. Irrespectively of the cube size, there is a tensile zone at the surface, which is around 1/5 of the cube size. At point A, due to drying there are high compressive stresses in the core, and tensile stresses at the edges for all the cube sizes (Fig. 17). From stress profiles, it can be also observed that at the edges, concrete entered the post-peak regime, indicating microcracking. The highest compressive stresses are observed for 150 mm cube (around 1.6 MPa), but this sample also exhibits the most pronounced softening at the edges. In Fig. 18, the cross sectional distributions of relative humidity (top) and resulting stress state (bottom) are given. Similarly as observed in Fig. 17, the highest compressive stresses after 28 days of drying occur in the middle of the largest specimen. Cross-sectional stress profiles clearly deviate from linear elastic stress distribution at the surface of the specimens, which is especially visible for the smallest, i.e., "fastest drying", sample (indicated with red arrow). This also confirms that drying and the resulting relative humidity gradients cause microcracking at the surface of specimens.

From A to B, 150 mm cube exhibits the largest reduction of compressive stresses in the core. From B to C, there is a large reduction in compressive stresses for 50 mm cube (Fig. 17c), also seen through a sharp decrease in the splitting strength (Fig. 12). At, point D, 50 mm cube reached hygral equilibrium, with compressive stresses in the core being negligible (Fig. 17c), and a strength reaching that of CM sample (Fig. 12). 100 mm and 150 mm specimens (Fig. 17a and b) reach hygral equilibrium only after longer exposure time (Points E and F). This is also in line with the trend observed for the measured splitting tensile

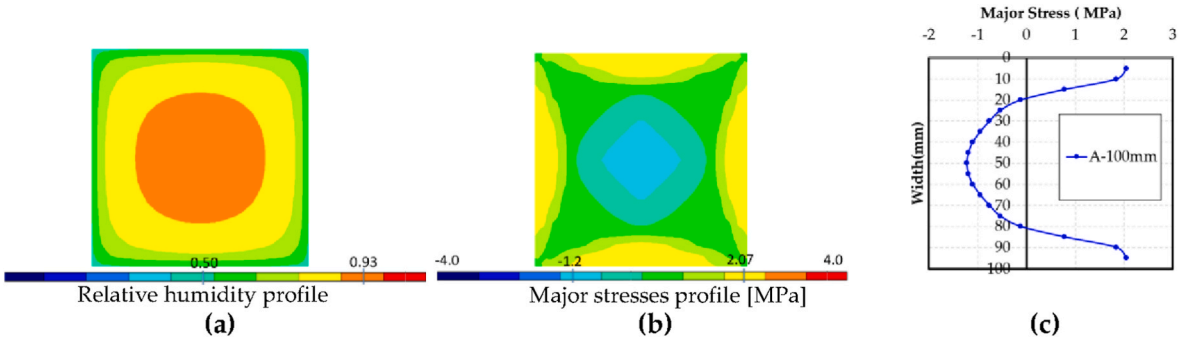

Fig. 13. **(a)** Relative humidity after 28 days of drying and resulting stress profile in 100 mm cube sample along **(b)** its cross section and **(c)** vertical mid-section (corresponding to Point A as labelled in Fig. 12).

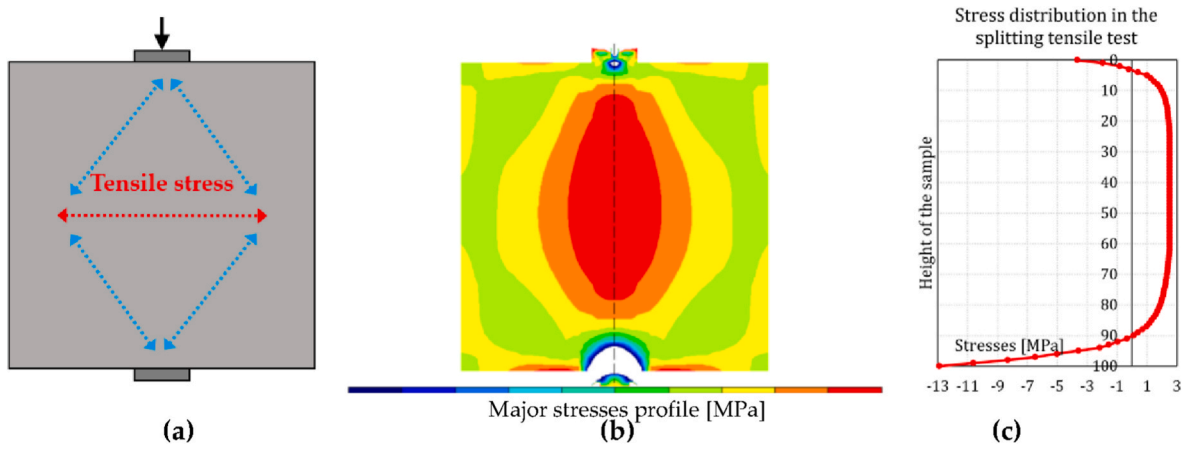

Fig. 14. Splitting tensile test on a cube **(a)** Mechanical scheme **(b)** Major stress contours over cross section **(c)** stress profile in the middle.

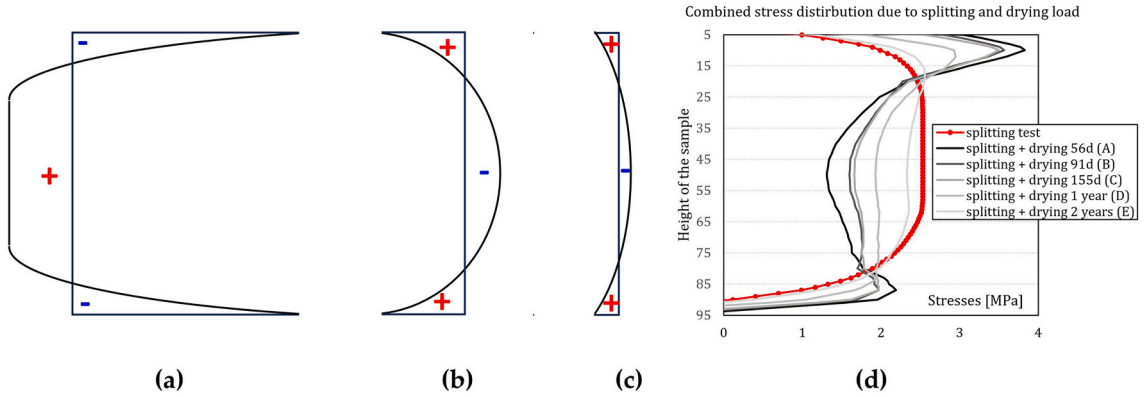

Fig. 15. Sketch of a stress profile due to **(a)** splitting test **(b)** drying at early period **(c)** drying at later period; **(d)** combination of stresses due to splitting and drying over time in 100 mm cube.

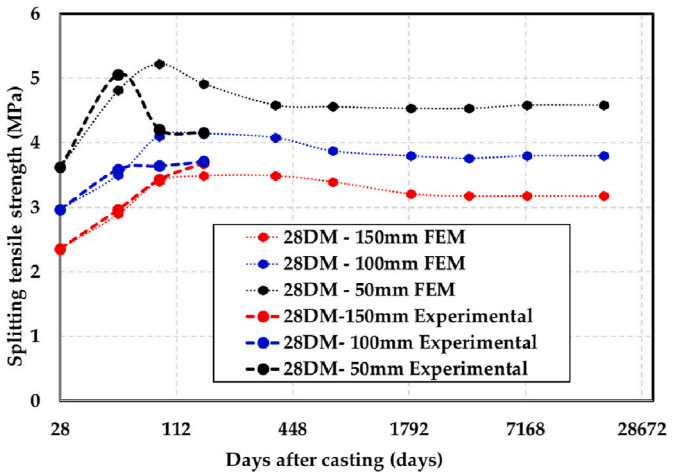

Fig. 16. Development of Splitting tensile strength of NSC with time.

strength in the experiments. In these samples, numerically it is observed that the apparent strength could be higher than the actual strength for a considerable duration of time (e.g. several years). Even though numerically some microcracking is observed at the surface of cubes due to drying, it is not significantly reducing the final splitting tensile strength. After reaching the hygral equilibrium, samples exposed to drying reached the same strength as constantly cured ones (Fig. 12).

4.4.2. *Direct tension test*

Similar to the splitting tensile tests, the trend of the direct tensile strength development is simulated for NSC until the period of 50 years. Unlike with splitting tensile strength for NSC, the drying conditions and resulting eigen-stresses can cause permanent reduction of the measured properties (Fig. 19a). Similar effect is also observed for HSC, in which eigenstresses and microcracking has even larger influence on the final measured strength. Beside permanent losses, it is observed that drying after moist curing of 28 days leads to temporary reduction of measured direct tensile strength for both the NSC and HSC which is especially pronounced in the early testing age. Drying induced hygral gradients create additional tensile stresses at the surface, on top of those caused by mechanical load. As a result, the failure load of the specimen is reduced. This is in line with earlier observations from Hordijk (1991) stating that curing conditions and drying time of the specimens, and therefore the moisture state of concrete, have significant influence on fracture mechanics parameters under direct tension. As the drying progresses and the specimen attains moisture equilibrium, tensile stresses at the surface are reduced, resulting in the gradual increase of the measured direct tensile strength.

Due to the relatively slow drying of the HSC owing to its lower film and diffusion coefficient (Table 5), the tensile stresses due to drying in HSC are retained for longer compared to NSC sample. At 38 days (point A), there are high tensile stresses at the surface for both NSC and HSC (Fig. 19b), while at 56 days (point B), the tensile stresses reduce considerably for NSC, which is not the case for HSC that shows further reduction of measured strength.

Numerically observed trend for the direct tensile strength is

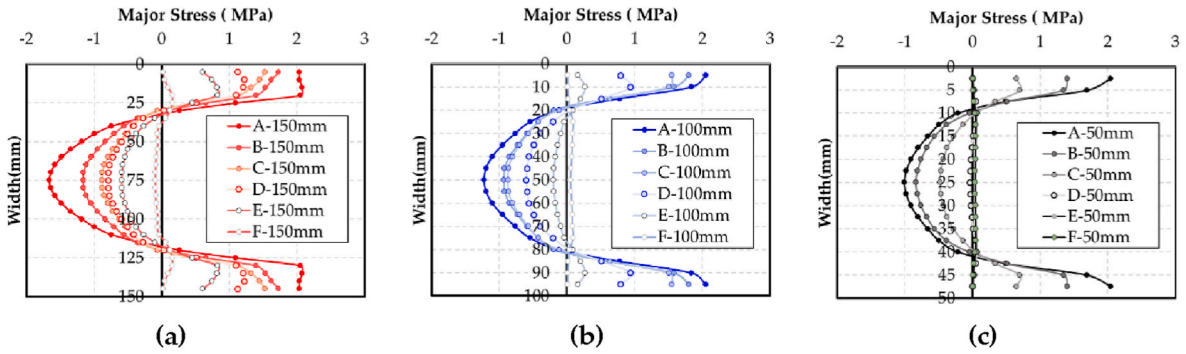

Fig. 17. Stress profiles across the cross section for different size specimens **(a)** 150 mm **(b)** 100 mm **(c)** 50 mm, for A, B, C, D, E and F profiles as labelled in Fig. 12.

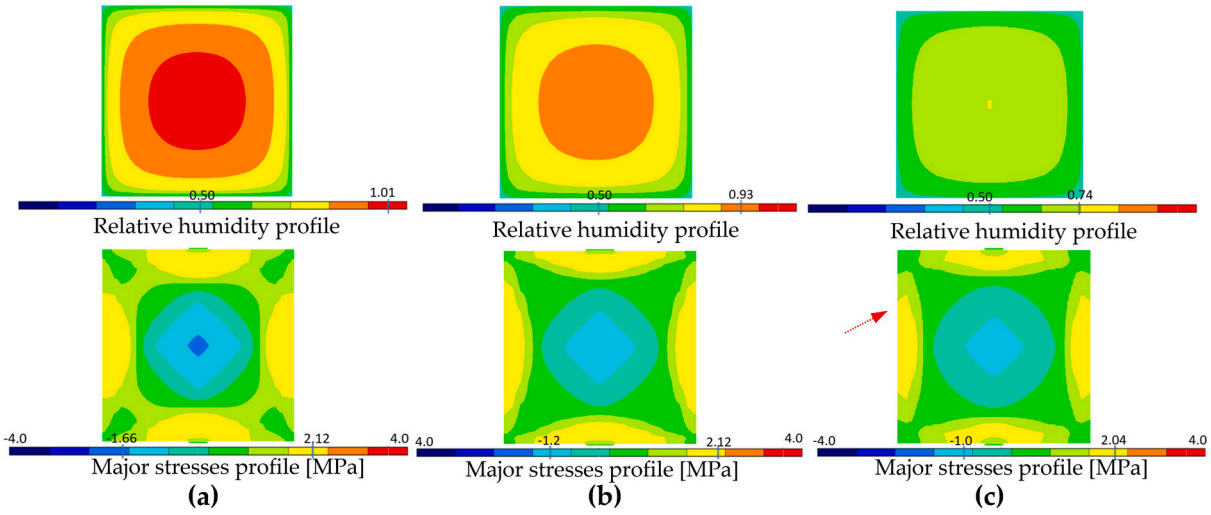

Fig. 18. Relative humidity (top) and corresponding major stress contours (bottom) after 28 days of drying (Point A as labelled in Fig. 12) for different size specimens **(a)** 150 mm, **(b)** 100 mm and **(c)** 50 mm.

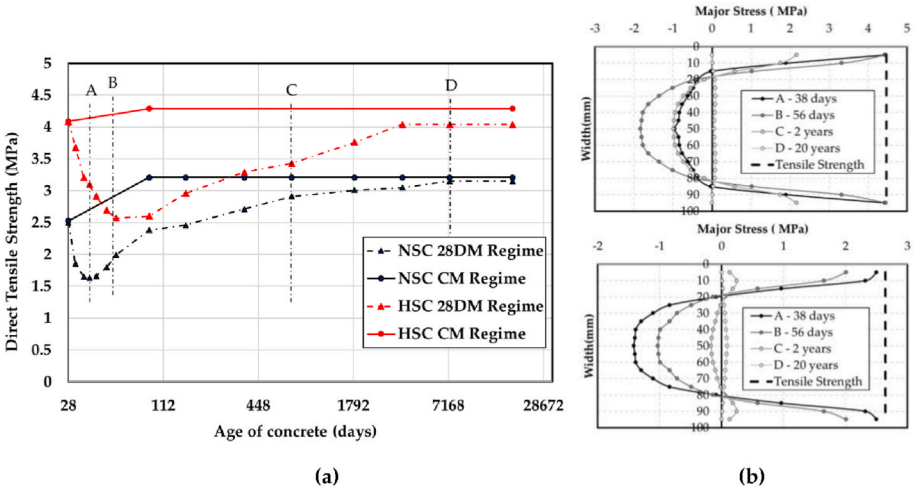

Fig. 19. **(a)** Apparent and "real" direct tensile strength over time for Normal Strength concrete (NSC) and High Strength Concrete (HSC) and **(b)** Major stress profile across the cross section for the various time intervals labelled in Fig. 21 for HSC specimens (top) NSC (bottom).

comparable to the results obtained by Bonzel (Bonzel and Walz, 1970) (Fig. 20a). A model with an imperfection in the centre is simulated to directly compare to Bonzel's results (Fig. 20b). In Bonzel's study, cylindrical specimens of 300 mm height and 150 mm diameter are used. As mentioned earlier, due to the difficulty in simulating cylinders for tensile tests, cubes are used after verifying that they have almost similar humidity profile as the cylinders (Fig. 11). In order to make a proper comparison with the results of Bonzel (Bonzel and Walz, 1970), direct tensile test is simulated using a 150 mm cube. It can be observed that in both cases, the general trend is the same with a drop until 42 days followed by an increasing trend. Both numerical and experimental results show that, opposite to the splitting tensile test, if measured before

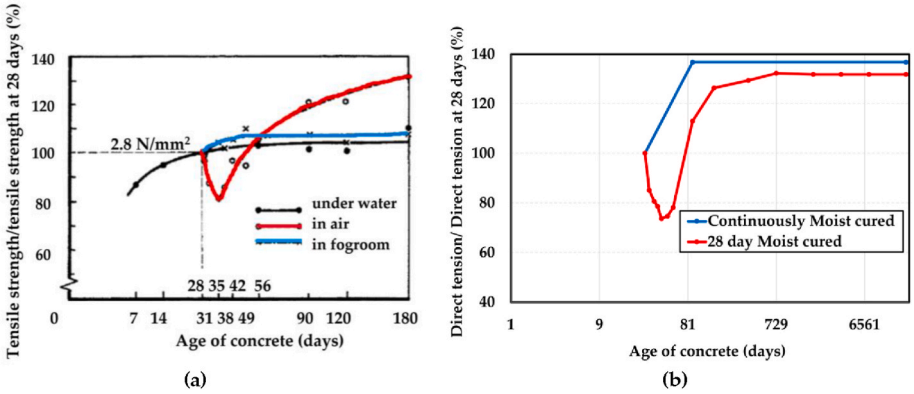

Fig. 20. Comparison of the direct tensile trend of **(a)** current simulation using FEMMASSE and **(b)** trend from the study of Bonzel (Bonzel and Walz, 1970).

reaching hygral equilibrium, direct tensile strength might be around 20–25% underestimated.

Bonzel and Walz (1970) also found a significant difference in tensile strength under wet condition, being lower compared to drying conditions, which is not observed in the model. Wittmann et al. (2007) explained this by surface energy of the solid skeleton being influenced by the thickness of adsorbed liquid films. When water is adsorbed on the surface of the nano-structure, the surface energy of the solid skeleton is reduced, the material expands and the strength of concrete decreases. Note that in simulations, this phenomenon is not considered. The input strength in the current simulation, is assumed to be constant after 91 days, which is in line with the water and fog room cured samples from Bonzel and Walz (1970).

4.4.3. Flexural test

In the flexural test set up, there are tensile stresses at the bottom surface, which coincide with the tensile stresses due to drying. As a result, the measured flexural tensile strength is reduced due to eigen-stresses, and the general trend obtained is similar to that of direct tensile strength. As the drying progresses, the specimen attains moisture equilibrium resulting in reduced tensile stresses at the surface and consequently an increase in measured flexural strength (Fig. 21). The period of increasing and decrease differs for the NSC and HSC specimens in the similar way like the direct tensile strength. Similar to the direct tensile test, depending on moment of testing, the "real" flexural strength might be significantly underestimated if the role of eigen-stresses is not considered.

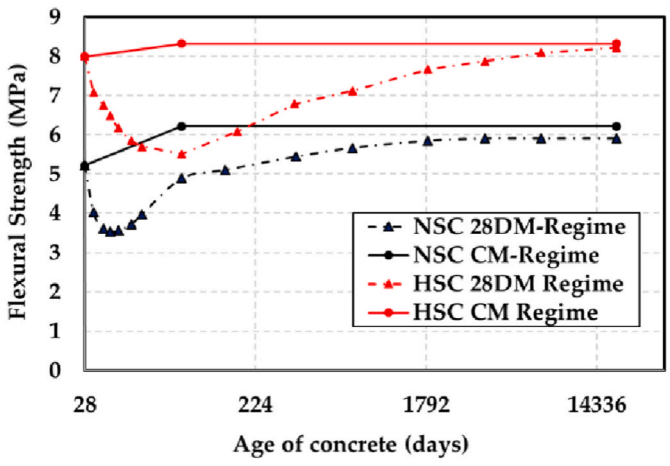

Fig. 21. Development of (apparent) flexural strength with age for NSC and HSC specimen.

5. General discussion

This paper highlights the relevance of testing conditions (i.e saturated, semi-saturated and dry) and the role of eigenstresses on the measured/apparent mechanical properties. Especially for semi-saturated conditions, the drying gradient (i.e. drying duration) and the size of the tested sample largely effects the measured mechanical properties.

Due to drying, the core of the sample is prestressed. In some testing configurations (e.g., the splitting tensile test), this might increase the apparent, "measured" strength. On the other hand, drying induces tensile stresses at the surface, and will result in seemingly lower tensile strength in the direct tension or flexural testing setup. In fact, these are not the different (intrinsic) tensile strengths: it is the maximum force measured in the sample that is different. Therefore, if this force is used directly to derive the tensile strength without considering the eigen stresses, the true material strength might be largely underestimated or overestimated, depending on the loading setup used, size of specimens and the specimen hygral conditions. Numerically it can be observed that by neglecting eigen-stresses on measured properties, and if tested at the same time, tensile strength derived from direct tensile test might be around 45–50% lower compared to the tensile strength derived from the splitting test, even though in both cases, the "real" material tensile strength is unchanged. Although surface microcracking is observed in the numerical study, it does not cause significant permanent losses in tensile splitting strength. Slightly higher permanent losses are observed for direct tensile and flexural tensile strength. Microcracks could not be detected experimentally.

Several limitations of this study apply which may explain the discrepancy between numerical and experimental results. First, drying is a three-dimensional effect, while in this study a two-dimensional numerical model has been used. This might have an influence on the magnitude of apparent strength increase or decrease. Unger and Eckardt (2011) compared the results of 2D and 3D modelling of the mechanical response of the concrete. For tensile failure, a 2D simulation results in a good agreement with experimental results, whereas a realistic simulation of compression tests requires a full 3D model. While our study is limited to modelling tensile failure, the drying process is a 3D phenomenon, and we recommend using a full 3D model in the future for better quantitative results. Furthermore, stress relaxation of eigen-stresses is neglected in the current simulations. However, eigen-stresses develop slowly and stress relaxation certainly occurs. Finally, given that the goal of this study was not to obtain accurate values, but to understand and explain the underlying phenomena, the hygral parameters used are either based on literature (for NSC) or on assumptions (for HSC). In reality, the hygral parameters need to be determined experimentally for each specific concrete.

Eigenstresses are difficult (so far impossible) to measure directly.

They can be derived from deformations (strain fields) within the sample and kinematic boundary conditions. Nonlinear Finite Element Method (FEM) and Finite Layer Method (FLM) are widely used for quantitative analysis of eigenstresses in both hardening and hardened concrete. In case hygral (or thermal) gradients are expected within the sample, the results should be analysed by numerical models, followed by inverse analysis by which the "real" material properties can be derived. In fact, the same methodology as commonly used for hygro-thermo-mechanical analysis of reinforced concrete structures should be applied in order to quantify the eigenstresses and derive the "real" material properties: (1) determine the strain fields caused by hygral (or thermal) gradients in the specimen; (2) once these strain fields and the kinematic boundary conditions of the mechanical tests are known, non-linear elastic stress analyses should be carried out; (3) obtained resistance (failure load) corresponds to the experimental result, from which the "real" material property should be determined by inverse analysis. An example of such analysis is summarized in the previous section. Alternatively, (semi-) analytical approaches (Sorgner et al., 2023) can also be used to translate hygral profiles into hygral eigenstrains, and resulting eigenstresses. These eigenstrains should then be split up into eigen-stretches, eigen--curvatures and eigen-distortion. For the presented material level tests, only the latter are restrained (at the cross-sectional scale) giving rise to non-linearly distributed self-equilibrated stresses. These stresses should be considered on top of those caused by mechanical loads. In order to avoid the effects of eigenstresses on measured properties, uniform moisture and hygral distribution have to be reached/assured before testing.

6. Conclusions

The main goal of this research was to understand the development of measured mechanical properties of ordinary concrete mixes of different strength grades and curing conditions over time considering the influence of eigen-stresses. Based on the presented results, the following conclusions can be drawn.

- From the combined experimental and numerical study, it might be observed that eigen-stresses play a significant role on the measured material strength.
- The elastic modulus of all the three grades of concrete is not affected by the varying curing regimes used in the study, unlike observed in alkali activated concretes (Prinsse et al., 2020).
- For Normal Strength Concrete (NSC) specimens, drying after 28 days moist curing (28DM regime) can increase the (apparent) splitting tensile strength and compressive strength temporarily up to 25% compared to CM samples. Also some decrease in splitting tensile strength compared to the "real strength" can be expected. This specific pattern is size dependent with the smaller cubes exhibiting it earlier compared to the larger cubes. In smaller samples the role of eigenstresses is higher, but in larger samples, eigen-stresses are longer present as it takes longer to reach the hygral equilibrium. If the role of eigen-stresses is not considered, measured strength could be higher than the "real" material strength for a considerable duration of time.
- The final resistance in the splitting tests is governed by the zone just below the surface, where both drying and splitting load cause tensile stresses, and magnitude of compressive stress in the core.
- UHPFRC requires longer time to reach the hygral equilibrium compared to NSC, so its real strength can be overestimated for significant time duration. A non-proportionality between measured compressive and splitting strength over time is observed, similarly as with 50 mm cubes made of NSC. Namely, in the same testing period, the measured compressive strength might be increasing whereas the tensile splitting strength might be decreasing. This is merely the effect of eigenstresses and not the real material strength increase/decrease.
- In case of the direct tensile strength and flexural strength, drying after a 28-day moist curing leads to a temporary reduction (around 20–25%) for both NSC and HSC specimens. The apparent tensile strength, until the hygral equilibrium is reached, is lower than the actual strength. By neglecting the eigen-stresses on measured properties, tensile strength derived from direct tensile or flexural test might be around half of that derived from the splitting test, even though in both cases, the "real" material tensile strength is unchanged.

Performed study has implications for several aspects. It shows the importance of considering properly eigen-stresses in the lab research: obtained data might be wrong if one does not consider eigen-stresses or does not take measures to avoid these stresses. The influence is present immediately after exposing samples to drying, therefore consistent preconditioning before testing is of utmost importance for reliable results. This is even more crucial when testing the small size samples and specimens at mortar and paste level. Is also important to understand the implication of the study when testing large scale samples, where eigen-stresses cannot be avoided, or when assessing existing structures, with cores usually being drilled to assess concrete properties. These structures are often exposed to wet-dry cycles, with no uniform moisture distribution. Therefore, it is important to understand the consequences of the specific test used, size of the sample, location of drilled core on obtained results. Finally, with development of new types of concretes, hybrid structures and advanced manufacturing (3D printing), eigen-stresses might play an even larger role due to the large fraction of paste used and layer-based fabrication in which the surfaces of the layers are exposed to the environment for a certain period before the next layer is applied.

Declaration of competing interest

The authors declare that they have no known competing financial interests or personal relationships that could have appeared to influence the work reported in this paper.

Data availability

Data will be made available on request.

Acknowledgments

Financial support by the Dutch Organization for Scientific Research (NWO) for the project 16814, "Optimization of interface behaviour for innovative hybrid concrete structures," is gratefully acknowledged by the authors.

References

Alvaredo, A., 1995. Crack formation under hygral or thermal gradients. In: Proceedings of Fracture Mechanics of Concrete Structures. (FraMCoS2), Zürich, Switzerland, pp. 1423–1441, 2.
Asselanis, J.G., Aitcin, P.C., Mehta, P.K., 1989. Effect of curing conditions on the compressive strength and elastic modulus of very high-strength concrete. Cem. Concr. Aggregates 11–1, 80–83.
Bartlett, F.M., MacGregor, J.G.., 1994. Effect of moisture condition on concrete core strengths. ACI Mater. J. 91 (3), 227–236.
Bazant, Z.P., 1986. Creep and Shrinkage of Concrete, Mathematical Modeling. Fourth Rilem International Symposium, Illinois.
Bažant, Z.P., 2000. Size effect. Int. J. Solid Struct. 37, 69–80.
Bezemer, H., Awasthy, N., Luković, M., 2023. Multiscale analysis of long-term mechanical and durability behaviour of two alkali-activated slag-based types of concrete. Construct. Build. Mater. 407, 133507.
Birchall, J., Howard, A., Kendall, K., 1981. Flexural strength and porosity of cements. Nature 289, 388–390.
Bisschop, J., van Mier, J.G., 2008. Effect of aggregates and microcracks on the drying rate of cementitious composites. Cement Concr. Res. 38, 1190–1196.
Bonzel, J., 1970. In: Walz, K. (Ed.), Einfluss der Nachbehandlung und des Feuchtigkeitszustandes auf die Zugfestigkeit des Betons. Betontechnische Berichte 1970, pp. 99–132.

Bouquet, G., 2019. Effect of Relaxation on Eigenstresses and Microcracking in Concrete under Imposed Deformation. Ph. D thesis. Delft University of Technology.
Carpinteri, A., 1994. Fractal nature of material microstructure and size effects on apparent mechanical properties. Mech. Mater. 18, 89–101.
Carrasquillo, R.L., Nilson, A.H., Slate, F.O., 1981. Properties of high strength concrete subjected to Short term loads. ACI 78–5, 171–178.
Collins, F., Sanjayan, J., 2001. Microcracking and strength development of alkali activated slag concrete. Cement Concr. Compos. 23–4, 345–352.
Conroy-Jones, G.A., Barr, B.I.G., 2004. Effect of curing on the tensile strength of medium to high strength concrete. Mag. Concr. Res. 3–56, 151–158.
Grassl, P., Bažant, Z.P., 2009. Random lattice-particle simulation of statistical size effect in quasi-brittle structures failing at crack initiation. J. Eng. Mech. 135, 85–92.
Hameed, A.H., 2009. The effect of curing condition on compressive strength in high strength concrete. Diyala journal of engineering sciences 2–1, 35–48.
Hanson, J., 1968. Effects of curing and drying enviroments on splitting tensile strength of concrete. Journal Proceedings 65–7, 535–543.
Hillerborg, A., 1978. A Model for Fracture Analysis, *Report TVBM-3005*, Division of Building Materials. Lund Institute of Technology, Lund, Sweden.
Hordijk, D.A., 1991. Local Approach to Fatigue of Concrete. Ph. D thesis. Delft University and Technology.
Iravani, S., 1996. Mechanical properties of high-performance concrete. ACI Mater. J. 93 (5), 416–426.
Kocab, D.B.K., Misak, P., Zitt, P., Kralikova, Monika, 2017. Development of the Elastic Modulus of Concrete under Different Curing Conditions. Procedia Engineering, Czech Republic.
Lantsoght, E.O., van der Veen, C., De Boer, A., van der Ham, H., 2018. Long-term material and structural behavior of high-strength concrete cantilever bridge: results of 20 years monitoring. Struct. Concr. 19 (4), 1079–1091.
Liu, D., Šavija, B., Smith, G.E., Flewitt, P.E., Lowe, T., Schlangen, E., 2017. Towards understanding the influence of porosity on mechanical and fracture behaviour of quasi-brittle materials: experiments and modelling. Int. J. Fract. 205, 57–72.
Logan, A.W.C., Mirmiran, A., Rizkalla, S., Zia, P., 2009. Short term mechanical proprties of high strength concrete. ACI Mater. J. 106 (5), 413–418.
Luković, M., Aldi, Z., Liu, J., Blom, K., Ye, G., 2017a. Optimization of a geopolymer mixture for a reinforced cantilever concrete bench. In: The 9th International Symposium on Cement and Concrete. ISCC).
Luković, M., Ye, G., Schlangen, E., Van Breugel, K., 2017b. Moisture movement in cement-based repair systems monitored by X-ray absorption. Heron 62, 21.
Maruyama, I., Sasano, H., Nishioka, Y., Igarashi, G., 2014. Strength and Young's modulus change in concrete due to long-term drying and heating up to 90°C. Cement Concr. Res. 48–63.
Mehta, P.K., Monteiro, P.J., 2017. Concrete Microstructure, Properties and Materials.
Ozer, B., Ozkul, M.H., 2004. The influence of initial water curing on the strength development of ordinary Portland and pozzolanic cement concretes. Cement Concr. Res. 34 (1), 13–18.
Popovics, S., 1986. Effect of curing method and final moisture condition on compressive strength of concrete. ACI Journal 83 (4), 650–657.
Prinsse, S., Hordijk, D.A., Ye, G., Lagendijk, P., Luković, M., 2020. Time-dependent material properties and reinforced beams behavior of two alkali-activated types of concrete. Struct. Concr. 21 (2), 642–658.
Roelfstra, P., 1989. A Numerical Approach to Investigate the Properties of Concrete Numerical Concrete. EPFL-Lausanne. Thesis.
Saul, A., 1951. Principles underlying the steam curing of concrete at atmospheric pressure. Mag. Concr. Res. 2, 127–140.
Sorgner, M., Flores, R.D., Wang, H., Hellmich, C., Pichler, B.L., 2023. Hindered thermal warping triggers tensile cracking in the cores of compressed columns of a fire-loaded tunnel segment structure: efficiency and accuracy of beam theory prediction, compared to FEM. Applications in Engineering Science 14, 100128.
Soroka, H.B.I., 1994. Influence of specimen size on effect of curing regime on concrete compressive strength. J. Mater. Civ. Eng. 6.
Unger, J.F., Eckardt, S., 2011. Multiscale modeling of concrete: from mesoscale to macroscale. Arch. Comput. Methods Eng. 18, 341–393.
Van Vliet, M.R., Van Mier, J.G., 2000. Experimental investigation of size effect in concrete and sandstone under uniaxial tension. Eng. Fract. Mech. 65, 165–188.
Wang, P., Villmann, B., Han, X., Slowik, V., Zhao, T., 2021. Diffusion coefficient and infinitesimal shrinkage strain of a Strain-Hardening Cement-Based Composite (SHCC) determined by inverse analysis of experiments. Cement Concr. Compos. 124, 104259.
Wardhono, A., Gunasekara, C., Law, D.W., Setunge, S., 2017. Comparison of long term performance between alkali activated slag and fly ash geopolymer concretes. Construct. Build. Mater. 143, 272–279.
Wittmann, F., Sun, Z., Zhao, T., 2007. Strength and fracture energy of concrete in seawater. In: In Proceedings of the Fracture Mechanics of Concrete and Concrete Structures. FraMCoS6), Catania, Italy, pp. 17–22.
Zhang, Y., Hubler, M., 2020. Role of early drying cracks in the shrinkage size effect of cement paste. J. Eng. Mech. 146, 04020128.
Zhang, Y., Zhang, M., 2014. Transport properties in unsaturated cement-based materials–A review. Construct. Build. Mater. 72, 367–379.